Proceedings of the ASME 2013 International Mechanical Engineering Congress & Exposition
IMECE 2013
November 13-21, 2013, San Diego, California, USA

IMECE2013-63600

STATIC AND DYNAMIC ANALYSIS OF AIRCRAFT STRUCTURES BY COMPONENT-WISE APPROACH

E. Carrera
A. Pagani*, M. Petrolo

Department of Mechanical and Aerospace Engineering
Politecnico di Torino
Corso Duca degli Abruzzi 29, 10129 Torino, Italy

ABSTRACT

This paper proposes an advanced approach to the analysis of reinforced-shell aircraft structures. This approach, denoted as Component-Wise (CW), is developed by using the Carrera Unified Formulation (CUF). CUF is a hierarchical formulation allowing for the straightforward implementation of any-order one-dimensional (1D) beam theories. Lagrange-like polynomials are used to discretize the displacement field on the cross-section of each component of the structure. Depending on the geometrical and material characteristics of the component, the capabilities of the model can be enhanced and the computational costs can be kept low through smart discretization strategies. The global mathematical model of complex structures (e.g. wings or fuselages) is obtained by assembling each component model at the cross-section level. Next, a classical 1D finite element (FE) formulation is used to develop numerical applications. It is shown that MSC/PATRAN can be used as pre- and post-processor for the CW models, whereas MSC/NASTRAN DMAP alters can be used to solve both static and dynamic problems. A number of typical aeronautical structures are analyzed and CW results are compared to classical beam theories (Euler-Bernoulli and Timoshenko), refined models and classical solid/shell FE solutions from the commercial code MSC/NASTRAN. The results highlight the enhanced capabilities of the proposed formulation. In fact, the CW approach is clearly the natural tool to analyze wing structures, since it leads to results that can be only obtained through three-dimensional elasticity (solid) elements whose computational costs are at least one-order of magnitude higher than CW models.

INTRODUCTION

Primary aircraft structures are essentially reinforced thin shells [1]. These are so-called *semimonocoque* constructions which are obtained by assembling three main components: skins (or panels), longitudinal stiffening members (including spar caps) and transversal stiffeners (ribs). The free vibration analysis and the determination of stress/strain fields in these structural components are of prime interest for structural analysts. Many different approaches were developed in the first half of the last century. These are discussed in major reference books [1, 2] and more recently in [3]. Among these approaches the so-called Pure Semimonocoque (PS) (or "idealized semimonocoque") is the most popular, since it assumes constant shear into panels and shear webs. The main advantage of PS is that it leads to a system of linear algebraical equations. However the number of such equations rapidly increases for multi-bay box structures with high redundancy. The number of resulting equations (and redundancy) can be strongly reduced by coupling PS with assumptions from Euler-Bernoulli (Euler-Bernoulli Beam Model, EBBM) or Timoshenko (Timoshenko Beam Model, TBM) theories. This lead to the so-called Beam Semimonocoque (BS) approach. Many works are known to overcome limitations related

*Corresponding author, email: alfonso.pagani@polito.it

to constant shear hypotheses, see [4–8] as examples.

Due to the advent of computational methods, mostly FEM, the analysis of complex aircraft structures continued to be made using a combination of solids (3D), plates/shells (2D) and beams (1D). These were implemented first in NASTRAN codes. Many others commercial FE codes have been developed and used in aerospace industries. Nowadays FEM models with a number of unknowns (degrees of freedom, DOFs) close to 10^6 are widely used in common practise. The possible manner in which stringers, spar caps, spar webs, panels, ribs are introduced into FE mathematical models is part of the knowledge of structural analysts. A short discussion of this follows. A number of works have shown the necessity for a proper simulation of the stiffeners-panel "linkage". Kolli and Chandrashekhara [9] formulated an FE model with 9-node plate and 3-node beam elements. Gangadhara [10] carried out linear static analyzes of composite laminated shells using a combination of 8-node plate elements and 3-node beam elements. As far as dynamic analysis is concerned, Samanta and Mukhopadhyay [11] developed a new stiffened shell element and, subsequently, they used this element to determine natural frequencies and mode shapes of different stiffened structures. In [12], Thinh and Khoa developed a new 9-node rectangular stiffened plate element for the free vibration analysis of laminated stiffened plates based on Mindlin's deformation plate theory. Recently, Vörös [13] formulated a new plate/shell stiffener element. In Vörös' theory, the stiffener element is developed by means of a general beam theory, which includes the constraint torsional warping effect and the second order terms of finite rotations.

The works mentioned so far show a clear interest in investigating FEM applications to reinforced-shell structures. In most of the articles in literature, such as those cited above, plates/shells and stiffeners are modeled as separate elements and a simulation of the stiffener-panel "linkage" is often necessary. Usually, beam nodes are connected to the shell element nodes via rigid fictitious links. This methodology presents some inconsistencies. The main problem is that the out-of-plane warping displacements in the stiffener section are neglected and the beam torsional rigidity is not correctly predicted.

The main aim of the present work is to introduce a new 1D formulation which is able to model reinforced-shell aircraft structures. The present *component-wise* (CW) approach deals with shells and stiffeners by means of a unique 1D formulation, with no need to introduce "fictitious links" to connect beam and shell elements. The CW approach has recently been exploited for the analysis of laminated composites [14] and it has proven to be able to model single fibers and related matrices, entire layers and whole multilayers. Furthermore, the CW models have shown their enhanced capabilities in dealing with both static [15] and free vibration [16] analysis of wing structures.

The present work is part of the framework of the one-dimensional Carrera Unified Formulation, CUF, which was recently proposed by the first author and his co-workers [17, 18]. Two classes of CUF 1D models were formulated: the Taylor-expansion class, hereafter referred to as TE, and the Lagrange-expansion class, hereafter referred to as LE. TE models exploit N-order Taylor-like polynomials to define the displacement field above the cross-section with N as a free parameter of the formulation. The strength of CUF TE models in dealing with arbitrary geometries, thin-walled structures and local effects were evident in static [19, 20] and free-vibration analysis [21, 22]. An important feature of TE models is that EBBM and TBM classical beam theories can be derived as degenerate cases of the linear Taylor-type expansion. Conversely, the LE class is based on Lagrange-like polynomials to discretize the cross-section displacement field and LE models have only pure displacement variables. Recently, static analyses on isotropic [18] and composite structures [23] have revealed the strength of LE models in dealing with open cross-sections, arbitrary boundary conditions and obtaining Layer-Wise descriptions of the 1D model. In the following a brief overview on CUF is proposed and the CW approach is described. Next, some examples are addresses. Finally, the main conclusions are outlined.

PRELIMINARIES

The notation assumed in this paper is hereafter introduced. The adopted coordinate frame is presented in Fig. 1. Let us introduce the transposed displacement vector,

$$\mathbf{u}(x,y,z) = \left\{ u_x \; u_y \; u_z \right\}^T \tag{1}$$

The cross-section of the structure is Ω, and the beam boundaries

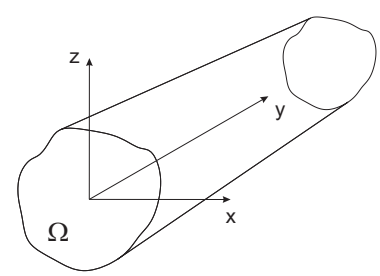

FIGURE 1. COORDINATE FRAME OF THE BEAM MODEL

over y are $0 \leq y \leq L$. The stress, σ, and strain, ε, components are grouped as follows:

$$\begin{aligned} \sigma_p &= \left\{ \sigma_{zz} \; \sigma_{xx} \; \sigma_{zx} \right\}^T, \; \varepsilon_p = \left\{ \varepsilon_{zz} \; \varepsilon_{xx} \; \varepsilon_{zx} \right\}^T \\ \sigma_n &= \left\{ \sigma_{zy} \; \sigma_{xy} \; \sigma_{yy} \right\}^T, \; \varepsilon_n = \left\{ \varepsilon_{zy} \; \varepsilon_{xy} \; \varepsilon_{yy} \right\}^T \end{aligned} \tag{2}$$

The subscript "n" stands for terms lying on the cross-section, while "p" stands for terms lying on planes which are orthogonal to Ω. In the case of small displacements with respect to a characteristic dimension of Ω, linear strain - displacement relations can be used

$$\begin{aligned} \varepsilon_p &= D_p \mathbf{u} \\ \varepsilon_n &= D_n \mathbf{u} = (D_{n\Omega} + D_{ny})\mathbf{u} \end{aligned} \tag{3}$$

where D_p and D_n are linear differential operators. They can be found in [17]. Constitutive laws were exploited to obtain stress components,

$$\sigma = C\varepsilon \tag{4}$$

According to Eqn.s (2), Eqn. (4) becomes

$$\begin{aligned} \sigma_p &= \tilde{C}_{pp}\varepsilon_p + \tilde{C}_{pn}\varepsilon_n \\ \sigma_n &= \tilde{C}_{np}\varepsilon_p + \tilde{C}_{nn}\varepsilon_n \end{aligned} \tag{5}$$

The matrices $\tilde{C}_{pp}$, $\tilde{C}_{nn}$, $\tilde{C}_{pn}$, and $\tilde{C}_{np}$ contains the material coefficients. For the sake of brevity they are not reported here. They can be found in [24].

HIGHER-ORDER FINITE BEAM ELEMENTS

In the framework of the CUF, the displacement field above the cross-section is the expansion of generic functions, F_τ,

$$\mathbf{u}(x,y,z) = F_\tau(x,z)\mathbf{u}_\tau(y), \qquad \tau = 1,2,....,M \tag{6}$$

where F_τ vary over the cross-section. $\mathbf{u}_\tau$ is the displacement vector and M stands for the number of terms of the expansion. According to the Einstein notation, the repeated subscript, τ, indicates summation. The choice of F_τ determines the class of 1D CUF model that has to be adopted. Two cases are addressed in this paper: TE and CW/LE.

TE 1D models are based on polynomial expansions, $x^i\ z^j$, of the displacement field above the cross-section of the structure, where i and j are positive integers. For instance, the displacement field of the second-order ($N = 2$) TE model is expressed by

$$\begin{aligned} u_x &= u_{x_1} + x\,u_{x_2} + z\,u_{x_3} + x^2\,u_{x_4} + xz\,u_{x_5} + z^2\,u_{x_6} \\ u_y &= u_{y_1} + x\,u_{y_2} + z\,u_{y_3} + x^2\,u_{y_4} + xz\,u_{y_5} + z^2\,u_{y_6} \\ u_z &= u_{z_1} + x\,u_{z_2} + z\,u_{z_3} + x^2\,u_{z_4} + xz\,u_{z_5} + z^2\,u_{z_6} \end{aligned} \tag{7}$$

The order N of the expansion is arbitrary and defines the beam theory. N can be set as an input of the analysis.

For LE class, F_τ are Lagrange-like polynomials. In this work, three types of cross-section polynomial sets were adopted: four- (L3), four- (L4), and nine-point (L9) elements. The isoparametric formulation was exploited to deal with arbitrary shaped geometries. The L3, L4 and L9 interpolation functions are given in [25]. For instance, the L4 function is

$$F_\tau = \frac{1}{4}(1 + r\,r_\tau)(1 + s\,s_\tau) \qquad \tau = 1,2,3,4 \tag{8}$$

where r and s vary from -1 to $+1$, whereas r_τ and s_τ are the coordinates of the four points whose numbering and location in the natural coordinate frame are shown in Fig. 2a. Unlikely TE,

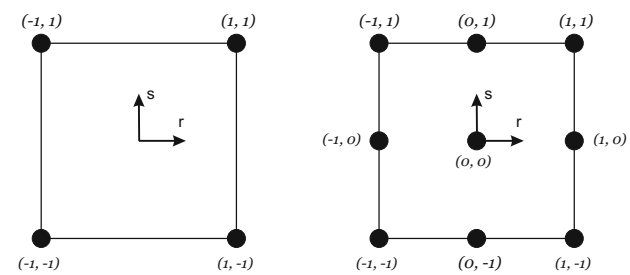

(a) Four-point element, L4 (b) Nine-point element, L9

FIGURE 2. CROSS-SECTION L-ELEMENTS IN NATURAL GEOMETRY

one of the most important feature of LE models is that they have only pure displacement degrees of freedom. More details about LE models can be found in the paper by Carrera and Petrolo [18].

For both TE and LE models, the FE approach was adopted to discretize the structure along the y-axis. This process is conducted via a classical finite element technique, where the displacement vector is given by

$$\mathbf{u}(x,y,z) = F_\tau(x,z)N_i(y)\mathbf{q}_{\tau i} \tag{9}$$

N_i stands for the shape functions and $\mathbf{q}_{\tau i}$ for the nodal displacement vector. For the sake of brevity, the shape functions are not reported here. They can be found in many books, for instance in [26]. Elements with four nodes (B4) were adopted in this work, that is, a cubic approximation along the y-axis was assumed.

The stiffness matrix of the elements, the mass matrix and the external loadings vector can be obtained via the principle of virtual displacements. For the sake of brevity, the derivation of the elemental matrices and the loading vector is not provided in this paper, but it can be found in [17]. For illustrative purpose,

TABLE 1. DISPLACEMENT VALUES, u_z, AT THE LOADED POINT AND NUMBER OF DEGREES OF FREEDOM FOR THE CONSIDERED STRUCTURAL CONFIGURATIONS OF THE THREE-BAY WING BOX

	Full Model		No Ribs Case		Open Mid-bay Case	
	$u_z \times 10^2$ m	DOFs	$u_z \times 10^2$ m	DOFs	$u_z \times 10^2$ m	DOFs
			MSC/NASTRAN			
SOLID/SHELL	1.412	100026	3.051	89400	1.963	89621
			Classical and Refined TE Beam Models			
EBBM	0.464	495	0.464	495	0.464	495
TBM	0.477	495	0.477	495	0.477	495
$N = 3$	0.793	1650	0.794	1650	0.873	1650
$N = 5$	1.108	3465	1.203	3465	1.500	3465
$N = 7$	1.251	5940	2.158	5940	1.745	5940
$N = 9$	1.325	9075	2.649	9075	1.836	9075
			CW			
	1.397	10750	2.981	10560	1.919	10446

the stiffness matrix in the form of fundamental nucleus is given in the following:

$$
\begin{aligned}
K^{ij\tau s} = & I_l^{ij} \triangleleft \left(D_{np}^T F_\tau I\right)\left[\tilde{C}_{np}\left(D_p F_s I\right) + \tilde{C}_{nn}\left(D_{np} F_s I\right)\right] + \\
& \left(D_p^T F_\tau I\right)\left[\tilde{C}_{pp}\left(D_p F_s I\right) + \tilde{C}_{pn}\left(D_{np} F_s I\right)\right] \triangleright_\Omega + \\
& I_l^{ij,y} \triangleleft \left[\left(D_{np}^T F_\tau I\right)\tilde{C}_{nn} + \left(D_p^T F_\tau I\right)\tilde{C}_{pn}\right] F_s \triangleright_\Omega I_{\Omega y} + \\
& I_l^{i,y j} I_{\Omega y} \triangleleft F_\tau \left[\tilde{C}_{np}\left(D_p F_s I\right) + \tilde{C}_{nn}\left(D_{np} F_s I\right)\right] \triangleright_\Omega + \\
& I_l^{i,y j,y} I_{\Omega y} \triangleleft F_\tau \tilde{C}_{nn} F_s \triangleright_\Omega I_{\Omega y}
\end{aligned}
\tag{10}
$$

where:

$$
I_{\Omega y} = \begin{bmatrix} 0 & 1 & 0 \\ 1 & 0 & 0 \\ 0 & 0 & 1 \end{bmatrix} \qquad \triangleleft \ldots \triangleright_\Omega = \int_\Omega \ldots \, d\Omega \tag{11}
$$

$$
\left(I_l^{ij} I_l^{ij,y}, I_l^{i,y j}, I_l^{i,y j,y}\right) = \int_l \left(N_i N_j, N_i N_{j,y}, N_{i,y} N_j, N_{i,y} N_{j,y}\right) dy \tag{12}
$$

It should be noted that $\mathbf{K}^{ij\tau s}$ does not depend either on the expansion order or on the choice of the F_τ expansion polynomials. These are the key-points of CUF which allows, with only nine FORTRAN statements, the implementation of any-order of multiple class theories.

The component-wise approach

The refined TE models described above are characterized by degrees of freedom (displacements and N-order derivatives of displacements) with a correspondence to the axis of the beam. The expansion can also be made by using only pure displacement values, e.g. by using Lagrange polynomials. The resulting LE can be used for the whole cross-section or can be introduced by dividing the cross-section into various sub-domains (see [18]). This characteristic allows us to separately model, for instance, stringers and panels. The LE formulation was used in this paper to implement CW models of reinforced-shell wing structures, as

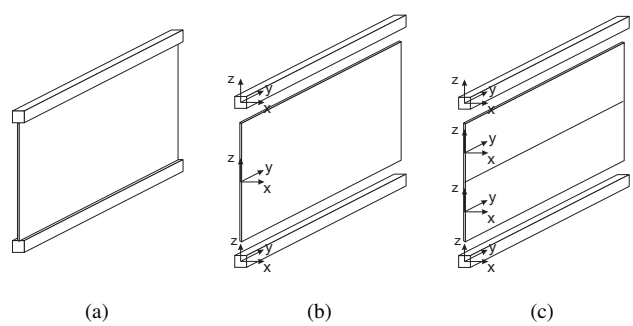

FIGURE 3. CW APPROACH THROUGH LE ELEMENTS

shown in Fig. 3a where a two-stringer spar is considered. Figure 3b shows a possible CW model of the spar where each component was modelled via one 1D LE element. Each LE element is then assembled above the cross-section to obtain the global stiffness matrix based on the 1D formulation. Since panels could not be reasonably modelled via a 1D formulation, 1D CW models can be refined by using several L-elements for one component. This aspect is shown in Fig. 3c where the panel is modelled via two 1D LE elements. By exploiting the present 1D formulation, the analysis capabilities of a structural model can be enhanced by 1. locally refining the LE discretization; 2. using higher-order LE elements (e.g. 4-node, 9-node, 16-node, etc.).

NUMERICAL RESULTS

Some examples are discussed in this section. First, the static analysis of a three-bay wing box is addressed. Next, free vibration analyses of a fuselage section and a complete wing are introduced. The results are compared both with classical beam theories and solid/shell elements of the commercial code MSC/NASTRAN. The attention is focused on the ability of the present CW formulation to foresee the effects due to both longitudinal and transverse stiffeners as well as open sections on thin-walled aerospace structures.

Static analysis of a three-bay wing box

The first analysis case was carried out on the three-bay wing box [15] for which PS and BS solutions were given in Rivello's book [2]. The considered structure is shown in Fig. 4a [2, chap. 11 p. 301], whereas Fig.s 4b and c show its variations. These examples highlight the capability of the present advanced 1D models to accurately describe the effects due to ribs and open sections. The structures consist of three wing boxes each with a length, l, equal to 0.5 m. The cross-section is a trapezium with a height $b = 1$ m. The two webs of the spars have a thickness of 1.6×10^{-3} m, whereas $h_1 = 0.16$ m and $h_2 = 0.08$ m. The top and the bottom panels have a thickness of 0.8×10^{-3} m, as well as ribs. The area of the stringers is $A_s = 8 \times 10^{-4}$ m^2. The wing is completely made of an aluminium alloy 2024, having $G/E = 0.4$. The cross-section in $y = 0$ was clamped and a point load, $F_z = 2 \times 10^4$ $[N]$, was applied at $[b, 2 \times l, h_2/2]$. Table 1 shows the vertical displacement values, u_z and the computational costs for each model implemented. Classical, increasing order TE and CW models are reported. The CW models were obtained by a combination of L4 and L9 elements. Results are validated by an MSC/NASTRAN model built both with solid and shell FE.

Figures 5, 6 and 7 show the span-wise variation of the axial and the shear stress components for the three different configurations. BS and PS solutions are provided for the full model of the three-bay wing box for comparison. The structure has three redundancies. Finally, Fig. 8 shows that the present CW model is able to detect the distribution of transverse stress components on ribs. The following remarks can be made:

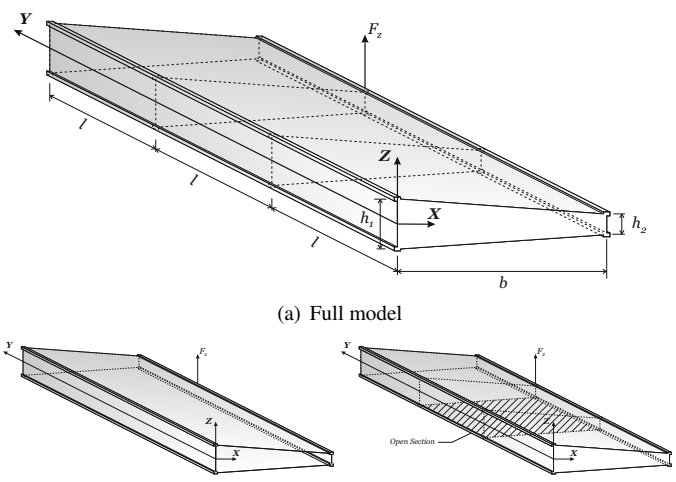

(a) Full model

(b) No ribs case

(c) Full model with open mid-bay

FIGURE 4. DIFFERENT STRUCTURAL CONFIGURATIONS OF THE THREE-BAY WING BOX

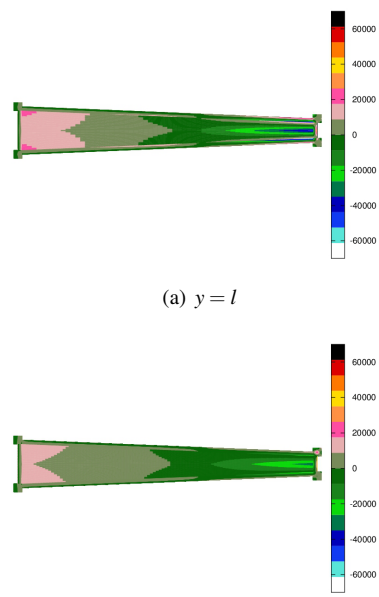

(a) $y = l$

(b) $y = 2 \times l$

FIGURE 8. TRANSVERSE STRESSES DISTRIBUTION, σ_{yz}, ON THE RIBS OF THE FULL MODEL OF THE THREE-BAY WING BOX, CW MODEL

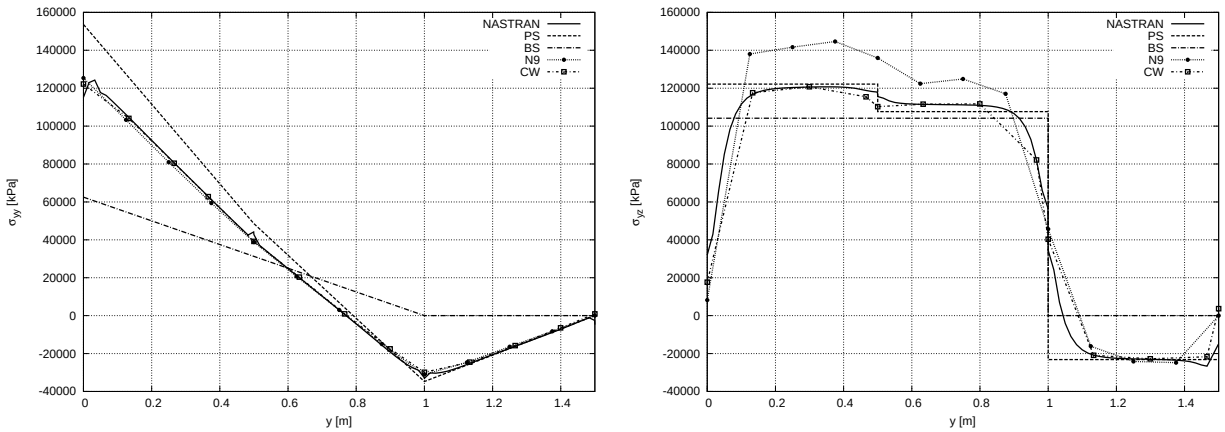

(a) Bottom right spar cap; σ_{yy} at $x = b$, $z = -\frac{h_2}{2}$

(b) Rear spar; σ_{yz} at $x = b$, $z = 0$

FIGURE 5. STRESS COMPONENTS DISTRIBUTION ALONG THE WING SPAN, FULL MODEL OF THE THREE-BAY WING BOX

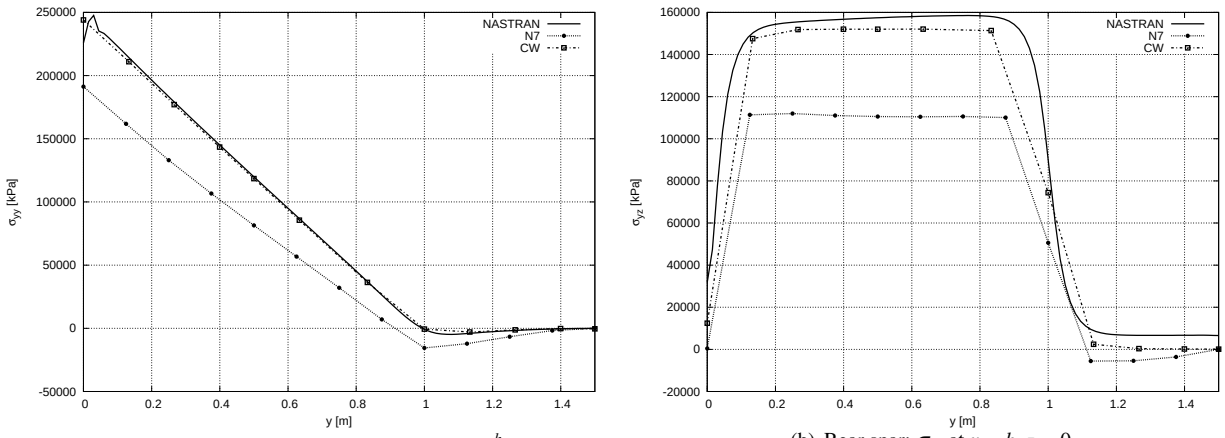

(a) Bottom right spar cap; σ_{yy} at $x = b$, $z = -\frac{h_2}{2}$

(b) Rear spar; σ_{yz} at $x = b$, $z = 0$

FIGURE 6. STRESS COMPONENTS DISTRIBUTION ALONG THE WING SPAN, THREE-BAY WING BOX WITH NO RIBS

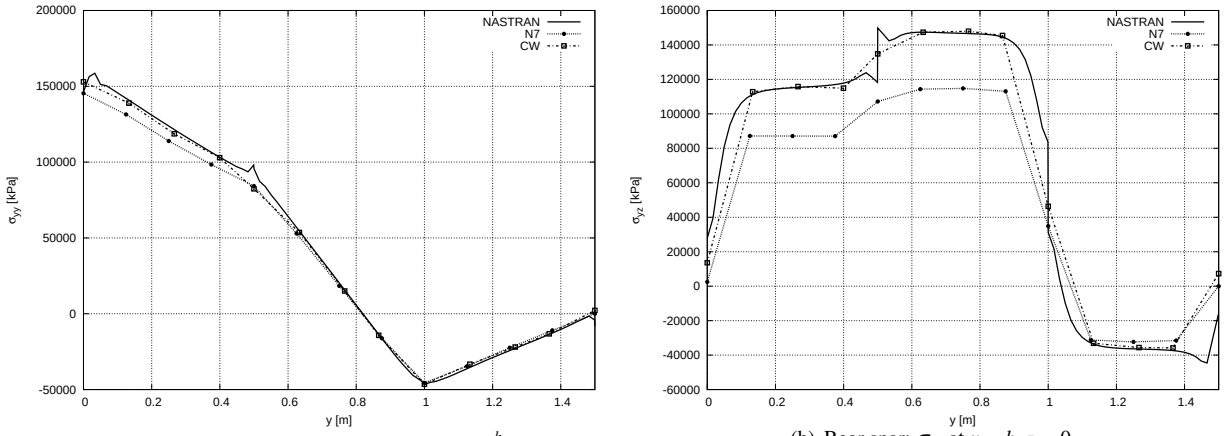

(a) Bottom right spar cap; σ_{yy} at $x = b$, $z = -\frac{h_2}{2}$

(b) Rear spar; σ_{yz} at $x = b$, $z = 0$

FIGURE 7. STRESS COMPONENTS DISTRIBUTION ALONG THE WING SPAN, THREE-BAY WING BOX WITH OPEN MID-BAY

1. CW/LE models correctly predict ribs and local effects, as they match the results obtained with solid/shell models.
2. Higher than sixth-order TE models are required to correctly predict the cross-section deformability.

Modal analysis of a fuselage section

The free vibration analysis of a fuselage section was carried out next. The cross-section of the fuselage is considered to be circular and it is shown in Fig. 9. The outer diameter, d, was set to 2 m, whereas the thickness, t, was 0.02 m. The length-to-diameter ratio, L/d, was taken to be equal to 10. The cylinder was made of an aluminium alloy with elastic modulus $E = 75 \times 10^3$ MPa and Poisson ratio $\nu = 0.33$. The fuselage was clamped at both its ends.

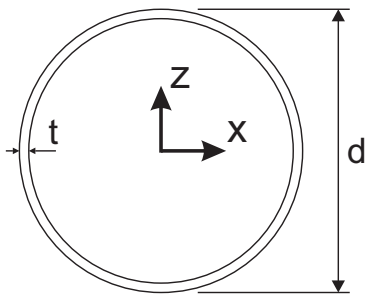

FIGURE 9. CIRCULAR CROSS-SECTION OF THE FUSELAGE

In Tab. 2 the main natural frequencies are shown and CUF models are compared to a MSC/NASTRAN model constructed with CQUAD4 shell elements. Both classical and refined TE models are given. The results by the CW model are reported in the last row. The CW model was obtained by discretizing the fuselage cross-section with 20 L9 Lagrange elements. Comparison between MSC/NASTRAN computational time and the presented method is also highlighted in Tab. 2.

Figure 10 shows the first bending, torsional and shell-like modal shapes by CW model. The following statements are worthy of careful study:

1. Classical and lower-order TE models are not able to describe the dynamic behavior of the fuselage structure.
2. Higher-order TE models are able to detect both global (bending, torsional) and local (shell-like) modes of the fuselage.
3. The proposed CW model of the thin-walled cylinder only detects bending and torsional natural frequencies. Local shell-like modes are not correctly described. This could be due to the high distortions that inflict LE elements for this particular problem. Improved results can be obtained by increasing the number of LE elements above the fuselage cross-section.

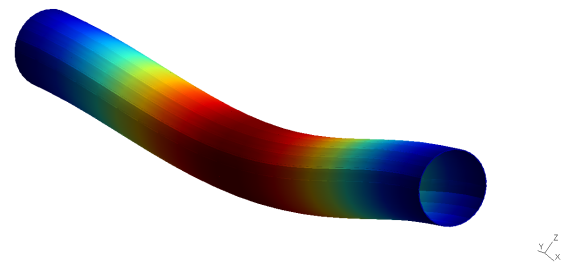

(a) Bending mode, 28.72 Hz

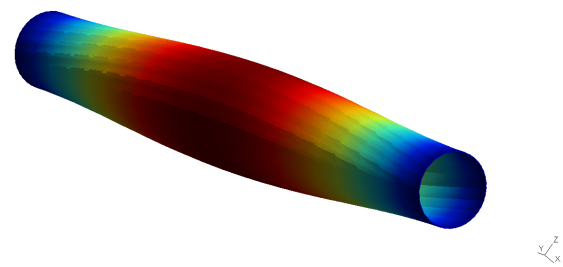

(b) Torsional mode, 80.71 Hz

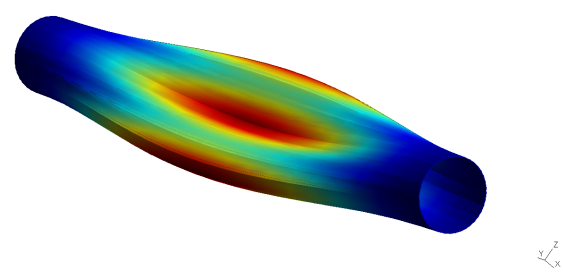

(c) Shell-like mode, 106.36 Hz

FIGURE 10. MAIN MODAL SHAPES OF THE FUSELAGE SECTION, CW MODEL

Modal analysis of a complete aircraft wing

The free vibration analysis of a complete aircraft wing was carried out for the final assessment. The cross-section of the wing is shown in Fig. 11. The NACA 2415 airfoil was used and two spar webs and four spar caps were added. The airfoil has the chord, c, equal to 1 m. The length, L, along the span direction is equal to 6 m. The thickness of the panels is 3×10^{-3} m, whereas the thickness of the spar webs is 5×10^{-3} m. The whole structure is made of the same isotropic material of the previous analysis case. The wing was clamped at the root. For the present wing structure, two different configurations were considered. *Configuration A* had no transverse stiffening members. In *Configuration B* the wing was divided into three equal bays, each separated by

TABLE 2. NATURAL FREQUENCIES (Hz) OF THE FUSELAGE SECTION AND COMPUTATIONAL TIME IN PERCENTAGE OF THE REFERENCE MODEL

Model	I Bending	II Bending	I Shell-like	II Shell-like	I Torsional	II Torsional	DOFs	Computational time
				MSC/NASTRAN				
SHELL	28.49	68.96	17.39	30.22	80.41	160.81	61440	100.00 %
				Classical and Refined TE Beam Models				
EBBM	32.60	88.08	-	-	-	-	93	0.0002 %
TBM	30.30	76.44	-	-	-	-	155	0.0006 %
$N = 1$	30.30	76.44	-	-	80.78	161.57	279	0.0021 %
$N = 2$	30.59	77.05	-	-	80.78	161.57	558	0.0082 %
$N = 3$	28.60	69.19	38.69	70.33	80.78	161.57	930	0.0229 %
$N = 4$	28.57	69.11	25.15	35.35	80.78	161.57	1395	0.0515 %
$N = 5$	28.57	69.11	20.48	32.22	80.78	161.57	1953	0.1010 %
				CW				
20 L9	28.72	69.44	106.36	109.67	80.71	161.43	7920	1.6617 %

*: not provided by the model

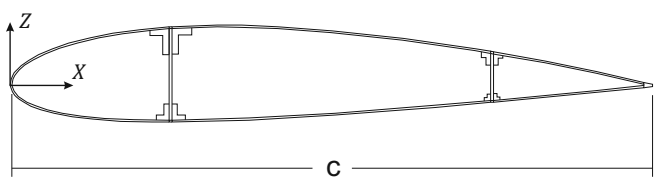

FIGURE 11. CROSS-SECTION OF THE WING

a rib with a thickness of 6×10^{-3} m.

Table 3 shows the main modal frequencies of both structural configurations of the wing. In this table, the results obtained through the CUF models are compared to those from classical beam theories and to those from SOLID models. In the last two rows of Tab. 3, the frequencies of the first two shell-like modes are stated. The following considerations hold.

1. The bending modes of the wing are correctly detected by both the lower-order and higher-order TE models.
2. As revealed by the previous numerical examples, at least a cubic expansion on the displacement field (TE $N = 3$) is necessary to correctly detect the torsional modes.
3. The CW models match the SOLID solutions, in fact, shell-like modes can be obtained by means of LE beam elements.
4. The computational effort of a higher-order beam model is significantly lower than the ones requested by solid models.

To deal with complex structures, such as the one considered in this section, the CW models were included into the commercial software MSC/NASTRAN, which was used to solve the eigenvalue problem through DMAP alters, and MSC/PATRAN

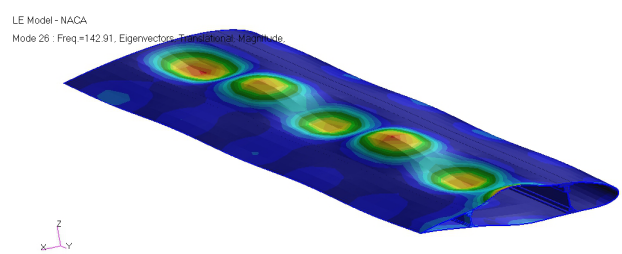

(a) Mode 26 (142.91 Hz)

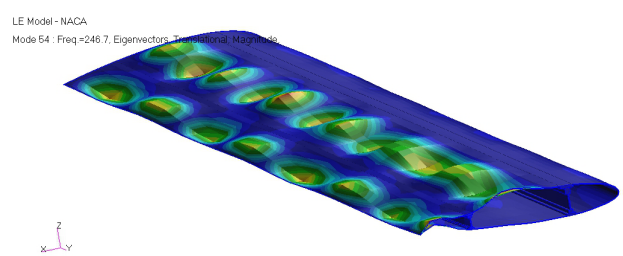

(b) Mode 54 (246.70 Hz)

FIGURE 12. SHELL-LIKE MODES OF THE WING (*CONFIGURATION A*) EVALUATED WITH THE CW MODEL

TABLE 3. GLOBAL AND LOCAL MODAL FREQUENCIES OF THE COMPLETE AIRCRAFT WING

	EBBM	TBM	$N=1$	$N=2$	$N=3$	CW	SOLID
				Configuration A			
DOFs	93	155	279	558	930	21312	186921
				Global Modes			
I Bending^{x*}	4.22	4.22	4.22	4.29	4.26	4.23	4.21
I Bending^{z}	22.10	21.82	21.82	21.95	21.87	21.76	21.69
II Bending^{x}	26.44	26.36	26.36	26.66	26.25	25.15	24.78
I Torsional	-	-	132.93	50.27	48.46	31.14	29.18
III Bending^{x}	73.91	73.35	73.35	73.99	71.64	59.26	56.12
				Local Modes			
I Shell-like	-	-	-	-	-	86.36	75.13
II Shell-like	-	-	-	-	-	88.94	73.85
				Configuration B			
DOFs	84	140	252	504	840	23976	171321
				Global Modes			
I Bending^{x*}	4.12	4.12	4.12	4.19	4.17	4.14	4.12
I Bending^{z}	21.56	21.30	21.30	21.50	21.42	21.28	21.22
II Bending^{x}	25.71	25.63	25.63	26.00	25.61	25.00	24.92
I Torsional	-	-	131.24	49.57	47.48	39.45	39.22
III Bending^{x}	71.44	70.90	70.90	71.80	69.49	64.84	63.88
				Local Modes			
I Shell-like	-	-	-	-	-	85.61	75.01
II Shell-like	-	-	-	-	-	91.54	78.61

* Bending$^{\xi}$: bending mode along the ξ-axis

was used for the post-processing of the CW model of the wing. Two shell-like modes evaluated by means of the CW model are shown in Fig. 12 for *Configuration A*.

CONCLUSIONS

This paper has considered and compared existing methods and recent approaches that exploit one-dimensional structural theories based on the Unified Formulation, which allows for the straightforward implementation of higher-order analysis without the need of extensive revisions of the model. The main conclusion to be drawn is that the present component-wise analysis appears to the authors to be the most convenient way, in terms of both accuracy and computational costs, in order to capture the global and local mechanical behavior of wing structures. However, particular attention has to be paid when discretizing structures with low radii of curvature. Additionally, the present CW approach allows us to build FE mathematical models by only using physical surfaces. This characteristic of CW models is a unique feature that makes this approach advantageous in a CAE/CAD scenario.

REFERENCES

[1] Bruhn, E. F., 1973. *Analysis and Design of Flight Vehicle Structures*. Tri-State Offset Company, Cincinnati, USA.

[2] Rivello, R. M., 1969. *Theory and analysis of flight structures*. McGraw-Hill, New York, USA.

[3] Carrera, E., 2011. *Fondamenti sul Calcolo di Strutture a Guscio Rinforzato per Veicoli Aerospaziali*. Levrotto & Bella, Torino, Italy.

[4] Cicala, P., 1946. "Sul calcolo delle strutture a guscio". *L'Aerotecnica,* **XXVI**(3), pp. 138–148. Part 1 of 4.

[5] Goodey, W. J., 1938. "A stressed skin problem". *Aircraft Engineering and Aerospace Technology,* **10**(1), pp. 11–13.

[6] Ebner, H., and Koller, H., 1937. "Zur berechnung des kraftverlaufes in versteiften zylindershalen". *Luftfahrtforschung,* **14**, pp. 607–626.

[7] Ebner, H., and Koller, H., 1938. "Ueber den kraftverlauf in längs und querversteiften scheiben". *Luftfahrtforschung,* **15**, pp. 527–542.

[8] Broglio, L., 1952. *Introduzione di un metodo generale per il calcolo delle strutture a guscio*. Istituto poligrafico dello Stato, Roma. Monografie scientifiche di aeronautica n. 1.

[9] Kolli, M., and Chandrashekhara, K., 1996. "Finite element analysis of stiffened laminated plates under transverse loading". *Composite Science and Technology,* **56**, pp. 1355–1361.

[10] Gangadhara Prusty, B., 2003. "Linear static analysis of hat stiffened laminated shells using finite elements". *Finite elements in analysis and design,* **39**, pp. 1125–1138.

[11] Samanta, A., and Mukhopadhyay, M., 2004. "Free vibration analysis of stiffened shells by the finite element technique". *European Journal of Mechanics - A/Solids,* **23**(1), pp. 159 – 179. DOI: 10.1016/j.euromechsol.2003.11.001.

[12] Thinh, T. I., and Khoa, N. N., 2008. "Free vibration analysis of stiffened laminated plates using a new stiffened element". *Technische Mechanik,* **28**(3–4), pp. 227–236.

[13] Vörös, G. M., 2007. "Finite element analysis of stiffened plates". *Periodica Polytechnica,* **51**(2), pp. 105–112.

[14] Carrera, E., Maiarú, M., and Petrolo, M., 2012. "Component-wise analysis of laminated anisotropic composites". *International Journal of Solids and Structures,* **49**, pp. 1839–1851. DOI: 10.1016/j.ijsolstr.2012.03.025.

[15] Carrera, E., Pagani, A., and Petrolo, M., 2013. "Classical, refined and component-wise theories for static analysis of reinforced-shell wing structures". *AIAA Journal*. In Press.

[16] Carrera, E., Pagani, A., and Petrolo, M., 2013. "Component-wise method applied to vibration of wing structures". *Journal of Applied Mechanics*. In Press.

[17] Carrera, E., Giunta, G., and Petrolo, M., 2011. *Beam Structures: Classical and Advanced Theories*. John Wiley & Sons. DOI: 10.1002/9781119978565.

[18] Carrera, E., and Petrolo, M., 2012. "Refined beam elements with only displacement variables and plate/shell capabilities". *Meccanica,* **47**(3), pp. 537–556. DOI: 10.1007/s11012-011-9466-5.

[19] Carrera, E., Giunta, G., Nali, P., and Petrolo, M., 2010. "Refined beam elements with arbitrary cross-section geometries". *Computers and Structures,* **88**(5–6), pp. 283–293. DOI: 10.1016/j.compstruc.2009.11.002.

[20] Carrera, E., Petrolo, M., and Zappino, E., 2012. "Performance of cuf approach to analyze the structural behavior of slender bodies". *Journal of Structural Engineering,* **138**(2), pp. 285–297. DOI: 10.1061/(ASCE)ST.1943-541X.0000402.

[21] Carrera, E., Petrolo, M., and Nali, P., 2011. "Unified formulation applied to free vibrations finite element analysis of beams with arbitrary section". *Shock and Vibrations,* **18**(3), pp. 485–502. DOI: 10.3233/SAV-2010-0528.

[22] Carrera, E., Petrolo, M., and Varello, A., 2012. "Advanced beam formulations for free vibration analysis of conventional and joined wings". *Journal of Aerospace Engineering,* **25**(2), pp. 282–293. DOI: 10.1061/(ASCE)AS.1943-5525.0000130.

[23] Carrera, E., and Petrolo, M., 2012. "Refined one-dimensional formulations for laminated structure analysis". *AIAA Journal,* **50**(1), pp. 176–189. DOI: 10.2514/1.J051219.

[24] Washizu, K., 1968. *Variational Methods in Elasticity and Plasticity*. Pergamon, Oxford.

[25] Oñate, E., 2009. *Structural Analysis with the Finite Element Method: Linear Statics, Volume 1*. Springer.

[26] Bathe, K. J., 1996. *Finite element procedure*. Prentice hall.